Published February 2, 2004

WIP Regulates Signaling via the High Affinity Receptor for Immunoglobulin E in Mast Cells

Alexander Kettner,[1] Lalit Kumar,[1] Inés M. Antón,[3] Yoji Sasahara,[1] Miguel de la Fuente,[1] Vadim I. Pivniouk,[1] Hervé Falet,[2] John H. Hartwig,[2] and Raif S. Geha[1]

[1]*Division of Immunology, Children's Hospital and* [2]*Division of Hematology, Brigham and Women's Hospital, Department of Pediatrics and Department of Medicine, Harvard Medical School, Boston, MA 02115*
[3]*Department of Clinical and Biological Sciences, University of Turin, 10043 Orbassano, Italy*

Abstract

Wiskott-Aldrich syndrome protein–interacting protein (WIP) stabilizes actin filaments and is important for immunoreceptor-mediated signal transduction leading to actin cytoskeleton rearrangement in T and B cells. Here we report a role for WIP in signaling pathways downstream of the high affinity receptor for immunoglobulin (Ig)E (FcϵRI) in mast cells. WIP-deficient bone marrow–derived mast cells (BMMCs) were impaired in their capacity to degranulate and secrete interleukin 6 after FcϵRI ligation. Calcium mobilization, phosphorylation of Syk, phospholipase C-g2, and c-Jun NH_2-terminal kinase were markedly decreased in WIP-deficient BMMCs. WIP was found to associate with Syk after FcϵRI ligation and to inhibit Syk degradation as evidenced by markedly diminished Syk levels in WIP-deficient BMMCs. WIP-deficient BMMCs exhibited no apparent defect in their subcortical actin network and were normal in their ability to form protrusions when exposed to an IgE-coated surface. However, the kinetics of actin changes and the cell shape changes that follow FcϵRI signaling were altered in WIP-deficient BMMCs. These results suggest that WIP regulates FcϵRI-mediated mast cell activation by regulating Syk levels and actin cytoskeleton rearrangement.

Key words: signal transduction • WIP • WASP • Wiskott-Aldrich syndrome • cytoskeleton

Introduction

Wiskott-Aldrich syndrome (WAS), an X-linked immunodeficiency, is caused by mutations in the gene encoding the WAS protein (WASP; 1). Hematopoietic cells from WAS patients show abnormalities in response to surface receptor–induced activation and in cytoskeletal function (2–6). These studies, together with the results from WASP-deficient mice, indicate that WASP functions as a scaffold or adaptor protein that regulates actin cytoskeleton reorganization and transcriptional activity (7, 8). The WASP-interacting protein (WIP) binds to the NH_2-terminal WH1 domain of WASP within a region that is frequently mutated in patients with WAS (9, 10). Point mutations within this region abrogate the binding of WASP to WIP (11). Interaction of WIP with WASP has been demonstrated to be involved in the regulation of T cell activation (12). T cells from WIP-deficient mice are impaired in their ability to proliferate and secrete IL-2 in response to TCR stimulation and have an abnormal subcortical actin filament network (13). These results support an important role for WIP in regulating the activation-induced rearrangement of the actin cytoskeleton downstream of immunoreceptor stimulation. Both WIP and WASP are also expressed in mast cells. These cells bear on their surface the high affinity receptor for IgE (FcϵRI), a member of the multichain immune recognition receptors (14). Upon FcϵRI aggregation, immunoreceptor tyrosine-based activation motifs of the g and b subunits become phosphorylated by the Src family tyrosine kinase lyn and recruit the protein tyrosine kinase Syk, which in turn phosphorylates intracellular proteins such as LAT, phospholipase C (PLC)-γ, Vav, and the adaptor protein SLP-76 (15–18).

Mast cells undergo dramatic morphological changes upon IgE-dependent stimulation, which triggers the release

A. Kettner, L. Kumar, and I.M. Antón contributed equally to this work.

Address correspondence to Raif S. Geha, Division of Immunology, Harvard Medical School, 300 Longwood Avenue, Boston, MA 02115. Phone: (617) 355-7603; Fax: (617) 739-3145; email: raif.geha@tch.harvard.edu

Abbreviations used in this paper: BMMC, bone marrow–derived mast cell; HSA, human serum albumin; MAP, mitogen-activated protein; PLC, phospholipase C; WAS, Wiskott-Aldrich syndrome; WASP, WAS protein; WCM, WEHI-3–conditioned medium; WIP, WASP-interacting protein.

 J. Exp. Med. © The Rockefeller University Press • 0022-1007/2004/02/357/12 $8.00
Volume 199, Number 3, February 2, 2004 357–368
http://www.jem.org/cgi/doi/10.1084/jem.20030652

Published February 2, 2004

of vasoactive agents from preformed granules as well as the synthesis and release of lipid mediators and cytokines. FcεRI has been shown to interact directly with the actin cytoskeleton and rearrangement of the actin cytoskeleton is associated with degranulation (19–21). Cytochalasin D, an inhibitor for actin polymerization, has been shown to enhance granule exocytosis upon FcεRI ligation (21, 22).

We have used mast cells derived from WIP-deficient mice to examine the role of WIP in FcεRI signaling. We found that degranulation, IL-6 production, and actin cytoskeleton dynamics after FcεRI ligation were impaired in $WIP^{-/-}$ mast cells. WIP was found to associate with Syk after FcεRI ligation and to inhibit Syk degradation as evidenced by markedly diminished Syk levels in WIP-deficient bone marrow–derived mast cells (BMMCs). These results suggest that WIP regulates FcεRI-mediated mast cell activation by regulating Syk levels and actin cytoskeleton rearrangement.

Materials and Methods

Cells and Cell Culture. The generation of WIP-deficient mice has been described elsewhere (13). Bone marrow cells were obtained by flushing the femur and tibia bones of $WIP^{-/-}$ mice and from WT littermates and were cultured in WEHI-3–conditioned medium (WCM) as a source of IL-3 (23). After 3–5 wk of culture, ≥90% of the cells derived from the bone marrow of $WIP^{-/-}$ and WT mice were mast cells, as assessed for IgE binding by FACS® analysis. BMMCs were incubated with mouse IgE, biotinylated rat anti–mouse IgE, and streptavidin-CyChrome (all from BD Biosciences). Cells were analyzed on a FACSCalibur™ flow cytometer (Becton Dickinson).

Enumeration of Mast Cells in Ear Skin. Ears from $WIP^{-/-}$ ($n = 2$) and control mice ($n = 2$) were fixed in 2% paraformaldehyde and processed into 3-mm–thick, paraffin-embedded sections stained with toluidine blue. Slides were examined by light microscopy for determination of mast cell numbers. Mast cells in six randomly chosen fields were counted per slide (six slides total for both $WIP^{-/-}$ and control mice).

Blood Histamine Measurements. Mice were sensitized with 3 mg mouse IgE anti-DNP mAb SPE-7 (Sigma-Aldrich) by i.v. injection in the retro-orbital vein. 24 h later, the mice were challenged with i.v. injection of human serum albumin (HSA)-DNP (0.5 mg per mouse). Blood histamine levels were determined by competitive RIA (Immunotech) on 100 ml plasma 1.5 min after antigen challenge according to the manufacturer's instructions.

β-Hexosaminidase Release Assay. 10^6 BMMCs were incubated in WCM containing 2.5 mg/ml rat IgE for 1 h on ice. After washing, pellets were resuspended on ice in WCM containing 0.1, 1, and 10 mg/ml $F(ab')_2$ fragments of mouse anti–rat Igs (Jackson ImmunoResearch Laboratories) or 10 mM ionomycin and incubated at 37°C for 20 min. The reaction was stopped by centrifugation. The pellets were resuspended in their original volume and lysed with WCM containing 0.5% Triton X-100. Aliquots of supernatants and cell lysates were incubated in duplicates with substrate solution (1.3 mg/ml *p*-nitrophenyl-b-D-2-acetamido-2-deoxyglucopyranozide in 0.1 M citrate, pH 4.5). The percent release values for each experimental condition were calculated by the formula $[S/(S+P)] \times 100$, where S and P are the b-hexosaminidase contents of the supernatant (S) and pellet (P) from each sample. The net release values were obtained by subtracting the OD for medium alone from S and P.

Measurement of Intracellular Calcium. 10×10^6/ml BMMCs were preloaded for 1 h on ice with 5 or 10 mg/ml rat IgE and 1 mM of the calcium-sensitive dye indo 1-AM in calcium buffer (PBS, pH 7.4, supplemented with 5 mM glucose, 1 mM $CaCl_2$, 0.5 mM $MgCl_2$, 1 mg/ml BSA, 10 mM Hepes). Cells were washed twice with calcium buffer and resuspended to the original concentration. 300 ml of cells were analyzed for calcium mobilization in a spectrophotometer (LS50; PerkinElmer). Excitation wavelength was 354 nm and emission wavelengths were 405 and 485 nm. Receptor-mediated change in calcium concentration was monitored after the addition of 25 or 50 mg/ml $F(ab')_2$ anti–rat Ig. Values were plotted as ratio of fluorescence at 405 and 485 nm.

Measurement of IL-6 Production. 10^6 BMMCs preloaded for 1 h on ice with 2.5 mg/ml rat IgE were incubated with 1 mg/ml of $F(ab')_2$ anti–rat Ig for 24 h in WCM at 37°C. Supernatants were assayed for IL-6 using an ELISA kit (R&D Systems).

Western Blotting and Immunoprecipitation. WIP, Syk, and actin protein expression was examined by Western blotting using rabbit anti–WIP (9, 24), rabbit anti–Syk (Santa Cruz Biotechnology, Inc.), and actin mAb (Chemicon).

For immunoprecipitation experiments, BMMCs were preloaded for 1 h on ice with 2.5 mg/ml rat IgE, and then stimulated for 7 min at 37°C with 10 mg/ml $F(ab')_2$ anti–rat Ig in WCM. After centrifugation, cells were lysed for 15 min on ice in lysis buffer (50 mM Tris, pH 7.4, 150 mM NaCl, 1 mM EDTA, 1% NP-40 supplemented with the following protease inhibitors: 3 mM diisopropyl fluorophosphate [Sigma-Aldrich], 1 mM PMSF [Sigma-Aldrich], 50 mg/ml antipain, and Complete™ protease inhibitor cocktail [all from Roche Molecular Biochemicals] and the following phosphatase inhibitors: 0.5 mM Na_3VO_4 and 5 mM NaF). Clarified cell lysates were subjected to immunoprecipitation with antibody to Syk, PLC-γ2 (Santa Cruz Biotechnology, Inc.), or SLP-76 (25), and then probed with antiphosphotyrosine mAb PT-66 or 4G-10 (Sigma-Aldrich). WIP immunoprecipitates were probed with anti-Syk antibody. In some experiments, cells were incubated with calpeptin (Calbiochem), MG132 (Sigma-Aldrich), or both for 4 h before analysis.

Activated mitogen-activated protein (MAP) kinases were detected by immunoblotting cell lysates with phospho-protein–specific antibodies (phospho-ERK1/2; Santa Cruz Biotechnology, Inc.), phospho-SAPK/JNK, and phospho-p38 (both from New England Biolabs, Inc.). Immunoreactive bands were detected by enhanced chemiluminescence (Amersham Biosciences).

Northern Blot Analysis of Syk mRNA. Total RNA from BMMCs was prepared using Trizol reagent (Sigma-Aldrich). Northern blot analysis for Syk was performed using NorthernMax Kit (Ambion) and a rat Syk cDNA, provided by R. Siraganian (National Institutes of Health, Bethesda, MD).

Spreading on IgE-coated Glass Coverslips. Glass coverslips were coated with mouse monoclonal IgE anti-ovalbumin (provided by M. Kiniwa, Taiho Pharmaceutical Co. Ltd., Saitama, Japan) overnight at 4°C. 0.2×10^6/ml BMMCs were allowed to attach to the glass for 15, 30, and 60 min at 37°C. Unattached cells were washed off and cells were fixed with 2% formaldehyde and then counted to determine the fraction of adherent cells. When indicated, BMMCs were preincubated with cytochalasin D at 10 mM for 1 h on ice, washed twice, and resuspended in culture medium. BMMCs were counted under a Nikon Eclipse TE2000 microscope.

To determine the percentage of attached cells, BMMCs (0.3×10^6/well in WCM) were allowed to attach to IgE-coated glass coverslips in 24-well plates for 1 h at 37°C in quadruplicates. The

Published February 2, 2004

plate was then agitated to dislocate nonadherent cells and the supernatant was collected and cells were sedimented by centrifugation. The pellet as well as the adherent cells were then lysed in the same volume of PBS 0.1% Triton X-100. β-hexosaminidase content was determined as described above. Percent adherence was calculated by the formula $[A/(A+S)] \times 100$, where A and S are the β-hexosaminidase contents of the adherent cells (A) and cells in supernatant (S) from each sample.

Electron Microscopy. 0.2×10^6/ml BMMCs were allowed to attach to IgE-coated coverslips for 60 min at 37°C. Cytoskeletons of attached cells were prepared by extraction with 0.75% Triton X-100 in PHEM buffer containing protease inhibitors and 2 mM phalloidin as previously described (26). Extracted BMMCs were briefly washed in PHEM buffer (60 mM Pipes, 25 mM Hepes, 10 mM EGTA, and 2 mM $MgCl_2$, pH 6.9) and fixed with 1% glutaraldehyde in PHEM buffer for 10 min. Cytoskeletons were washed trice with double distilled water just before freezing. Samples were rapid frozen, freeze dried, and rotary shadowed with 1.2 nm tantalum-tungsten followed by 2.5 nm carbon. Specimens were examined and photographed in a JEOL 1200-EX electron microscope using an accelerating voltage of 100 kV.

Determination of Cellular F-Actin. 10^6 BMMCs preloaded for 1 h on ice with 2.5 mg/ml rat IgE were incubated with 10 mg/ml $F(ab')_2$ anti–rat Ig for the indicated time in WCM at 37°C. Cells were immediately fixed for 10 min by adding 4% formaldehyde (2% final concentration). They were then permeabilized and stained in a single step with 0.1% Triton X-100 and 1 mg/ml phalloidin-TRITC in PHEM buffer for 40 min and analyzed by FACS®.

Measurement of Filament Ends. 10×10^6/ml BMMCs were preloaded for 1 h on ice with 2.5 mg/ml rat IgE in calcium buffer. Cells were washed twice in calcium buffer and resuspended at the concentration of 20×10^6/ml. Cells (10^6/ml in 50 μl) were activated by the addition of an equal volume of 20 mg/ml $F(ab')_2$ anti–rat IgE for 1, 2, 5, and 15 min. Resting and activated cells were extracted with 0.1% Triton in PHEM buffer containing protease inhibitors and 1 mM phallacidin. 185 ml of 100 mM KCl, 2 mM $MgCl_2$, 0.5 mM ATP, 0.1 mM EGTA, 0.5 mM DTT, and 10 mM Tris, pH 7.0, was then added and the polymerization rate assay was started by the addition of 15 ml monomeric pyrene-labeled rabbit skeletal muscle actin to a final concentration of 1 mM. Pyrene-actin fluorescence was recorded using a spectrofluorimeter (LS50; PerkinElmer). Excitation and emission wavelengths were 366 and 386 nm, respectively. Activity inhibited by 2 mM cytochalasin B is defined as barbed end actin assembly. Activity not inhibited by cytochalasin B is defined as pointed end actin assembly. The number of actin filament ends was determined as previously described (27). Initial barbed and pointed end addition rates in 1 mM actin solution are 10 and 1 monomers s^{-1}, respectively.

Time Lapse Video Microscopy. For degranulation on fibronectin, cells were preloaded with 2.5 mg/ml IgE and transferred at 0.2×10^6/ml into 24-well plates that contained glass coverslips that were coated with fibronectin at 10 mg/ml. Cells were allowed to sediment at room temperature for 10 min and then were transferred to 37°C for 20 min. Coverslips with adherent cells were briefly dipped in prewarmed WCM and then transferred to the warm stage of the Nikon Eclipse TE2000 microscope. Images were acquired with a CCD-300-RC charge-coupled device (Dage-MTI) at ×400. Frames were taken every 6 s for 15 min. After 1 min of recording, 1 mg/ml $F(ab')_2$ fragments of mouse anti–rat Ig was added.

Statistical Analysis and Densitometry. Statistical analyses of the data were performed with Prism software (version 3.0a). Blots were scanned and analyzed with NIH Image software (version 1.62). Results were expressed as fold induction over baseline and were normalized to signal for loading.

Results

BMMCs Develop Normally in the Absence of WIP. Mouse bone marrow cells cultured in the presence of IL-3 differentiate into mast cells (23). After 4 wk of culture in IL-3–containing WCM, a similar number and percentage of cells (~90%) from $WIP^{-/-}$ and WT mice differentiated to mast cells as evidenced by their capacity to bind IgE (Fig. 1 A). Furthermore, the same proportion of cells contained metachromatic granules when stained with toluidine blue (not depicted).

Lysates from WT and WIP-deficient cells were examined by Western blotting for expression of WIP. As shown in Fig. 1 B, only WT cells express WIP. The kinetics of cell growth and differentiation of $WIP^{-/-}$ and WT BMMCs were similar (not depicted). We also examined the number of tissue mast cells in $WIP^{-/-}$ mice. The number of mast cells in the ear skin of $WIP^{-/-}$ mice (16 ± 4 per high power field, $n = 6$) was comparable to that of controls (16 ± 3 per high power field, $n = 6$).

IgE-mediated Systemic Histamine Release Is Greatly Diminished in $WIP^{-/-}$ Mice. Adoptive transfer of IgE antibodies to normal mice primes them to undergo passive systemic anaphylactic reactions in response to intravenous challenge with specific antigen. IgE-mediated anaphylaxis is dependent both on mast cells and FcεRI signaling as it is dimin-

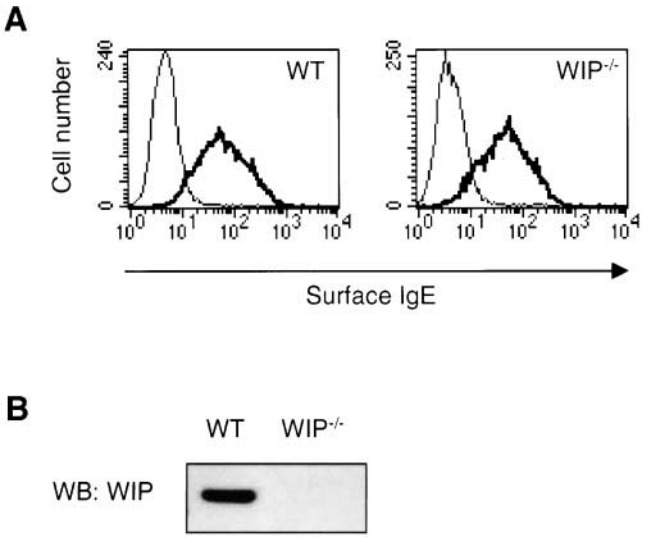

Figure 1. Characterization of in vitro–derived $WIP^{-/-}$ BMMCs. (A) IgE receptor expression on BMMCs form WT and $WIP^{-/-}$. Cells were treated with mouse IgE and then incubated with biotinylated anti-IgE and streptavidin-CyChrome (bold line). Control staining was with biotinylated anti-IgE and streptavidin-CyChrome alone (thin line). (B) WIP protein expression was assessed by immunoblotting after separation of proteins by SDS-PAGE.

Published February 2, 2004

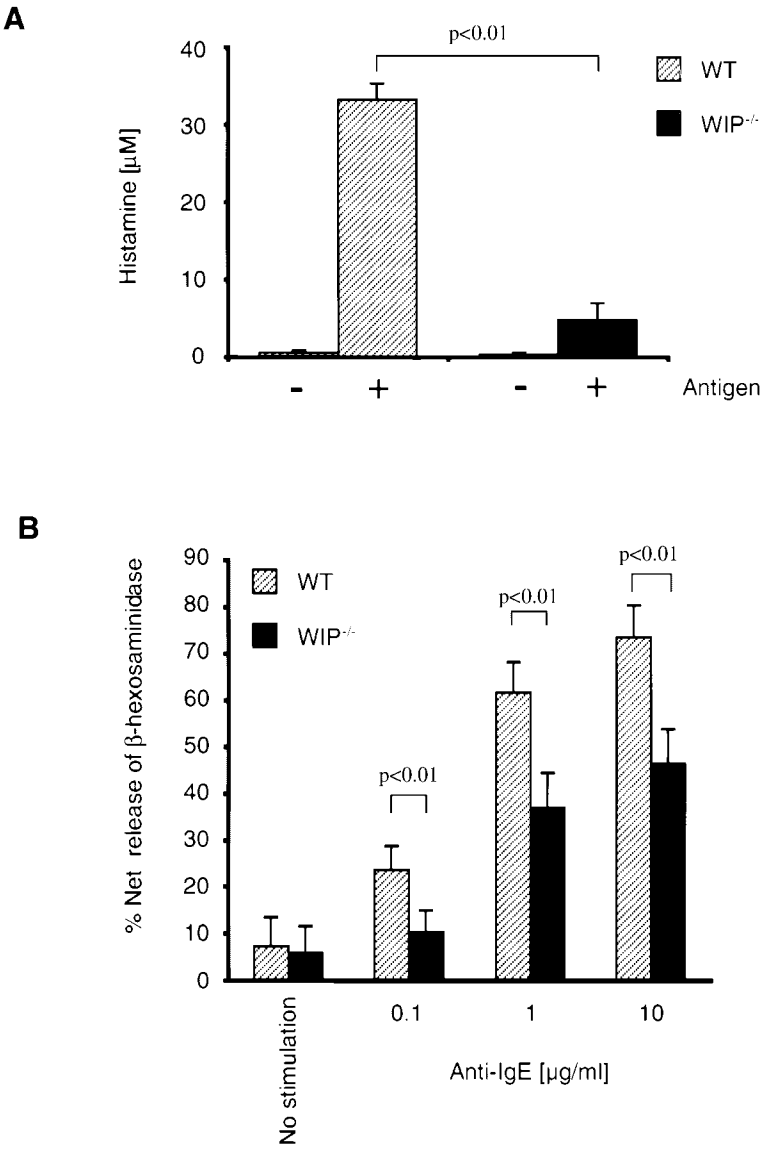

Figure 2. In vivo IgE-dependent histamine release and in vitro degranulation is diminished in WIP$^{-/-}$ mice. (A) WIP$^{-/-}$ mice and WT controls were sensitized with 3 mg IgE by i.v. injection in the retro-orbital vein. 24 h later the mice were challenged with i.v. injection of HSA-DNP. Blood histamine levels were determined by competitive RIA in plasma collected 1.5 min after antigen challenge. (B) IgE-mediated in vitro degranulation of WIP$^{-/-}$ BMMCs. Release of β-hexosaminidase. BMMCs preloaded with IgE were stimulated with F(ab′)$_2$ anti–rat Ig at indicated concentrations. Results represent mean ± SD of three experiments from two independently derived WT and WIP$^{-/-}$ cell lines, each analyzed in duplicates. Statistical analysis was performed using the Student's *t* test.

ished in mast cell–deficient W/W^v mice (28, 29), virtually absent in mast cell–deficient Sl/Sl^d mice (30), and dramatically reduced in FcεRIα-deficient mice (31). Dramatic increase of plasma concentration of histamine, a major vasoactive mediator released by activated mast cells and basophils, has been shown to correlate with systemic anaphylaxis (32). To evaluate whether expression of WIP is important in regulating IgE-dependent systemic release of histamine, we passively sensitized four WIP$^{-/-}$ mice and six control littermates with mouse IgE anti-DNP mAb. 24 h later, mice were challenged with DNP-HSA and plasma histamine concentration was determined before and 1.5 min after challenge with antigen (Fig. 2 A). Plasma histamine levels before antigen administration were comparable in WT and WIP$^{-/-}$ mice. After antigen challenge, the increase in plasma histamine concentration was dramatic in WT mice but minimal in WIP$^{-/-}$ mice (Fig. 2 A). This finding suggests that WIP is essential for IgE-mediated systemic anaphylaxis in mice.

IgE-dependent Release of β-Hexosaminidase of WIP-deficient Mast Cells. Next, we tested the capacity of mast cells derived from WIP$^{-/-}$ mice to release preformed mediators stored in their granules upon cross-linking of FcεRI-bound IgE by antigen in vitro. BMMCs derived from WT and WIP$^{-/-}$ mice were sensitized with rat IgE. FcεRI-bound IgE was cross-linked 1 h later with increasing concentrations of F(ab′)$_2$ anti–rat Ig and the release of the granular enzyme β-hexosaminidase was determined after 20 min of incubation. FcεRI-mediated release of β-hexosaminidase by WIP$^{-/-}$ BMMCs was significantly reduced at all concentrations of cross-linker used as compared with WT cells (Fig. 2 B). Furthermore, β-hexosaminidase release in WIP$^{-/-}$ BMMCs was suppressed to the same extent after 1, 2, 5, 10, 15, and 20 min at a single dose of cross-linking antibody (1 mg/ml) tested (not depicted). β-Hexosaminidase release was complete at 5 min and did not increase significantly thereafter for both cell types. Granule exocytosis induced by

Published February 2, 2004

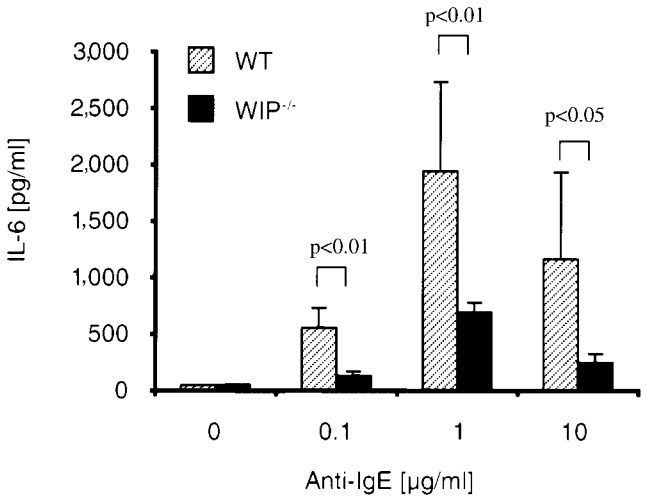

Figure 3. IgE-mediated IL-6 release of WIP$^{-/-}$ BMMCs. IL-6 release by BMMCs. BMMCs preloaded with IgE were incubated with F(ab′)$_2$ anti–rat Ig for 24 h. IL-6 release was determined by ELISA. Results represent mean ± SD of three experiments. Statistical analysis was performed using the Student's *t* test.

ionomycin was comparable in WT and WIP$^{-/-}$ cells, indicating that ionophore-induced granule secretion is normal in WIP$^{-/-}$ BMMCs (not depicted).

FcεRI-mediated IL-6 Production Is Impaired in WIP-deficient BMMCs. To assess the role of WIP in FcεRI-mediated cytokine production, IL-6 concentration was measured in cell culture supernatants of BMMCs 24 h after stimulation. WIP$^{-/-}$ BMMCs secreted markedly less IL-6 than WT controls at all concentrations of cross-linker used (Fig. 3).

Intracellular Calcium Concentration and Tyrosine Phosphorylation of PLC-γ2 after Cross-linking of FcεRI. Upon FcεRI cross-linking, PLC-γ becomes rapidly phosphorylated and activated to hydrolyze membrane phosphoinositides to generate IP_3, which initiates an increase in intracellular calcium. A rapid sustained increase in intracellular calcium levels is important for FcεRI-mediated degranulation and cytokine release in mast cells (33, 34). After FcεRI ligation, intracellular calcium levels in WIP$^{-/-}$ BMMCs rapidly increased but remained significantly below those observed in WT BMMCs throughout the 6-min observation period (Fig. 4 A). Similarly decreased calcium fluxes were still observed under conditions of higher FcεRI cross-linking (10 mg/ml rat IgE and 50 mg F(ab′)$_2$ anti–rat Ig).

Although BMMCs express both PLC-γ isoforms, it has been demonstrated that PLC-γ2 is crucial for mast cell degranulation and IL-6 secretion (35). Tyrosine phosphorylation of PLC-γ2 was markedly reduced in WIP$^{-/-}$ BMMCs after FcεRI ligation as compared with WT controls (Fig. 4 B). The decrease of PLC-γ2 tyrosine phosphorylation is not a consequence of a general failure to phosphorylate intracellular substrates as the pattern and intensity of global phosphorylation was the same in WT and WIP$^{-/-}$ BMMCs (not depicted). Moreover, SLP-76 that becomes rapidly tyrosine phosphorylated by Syk after FcεRI ligation was normally phosphorylated (Fig. 4 C).

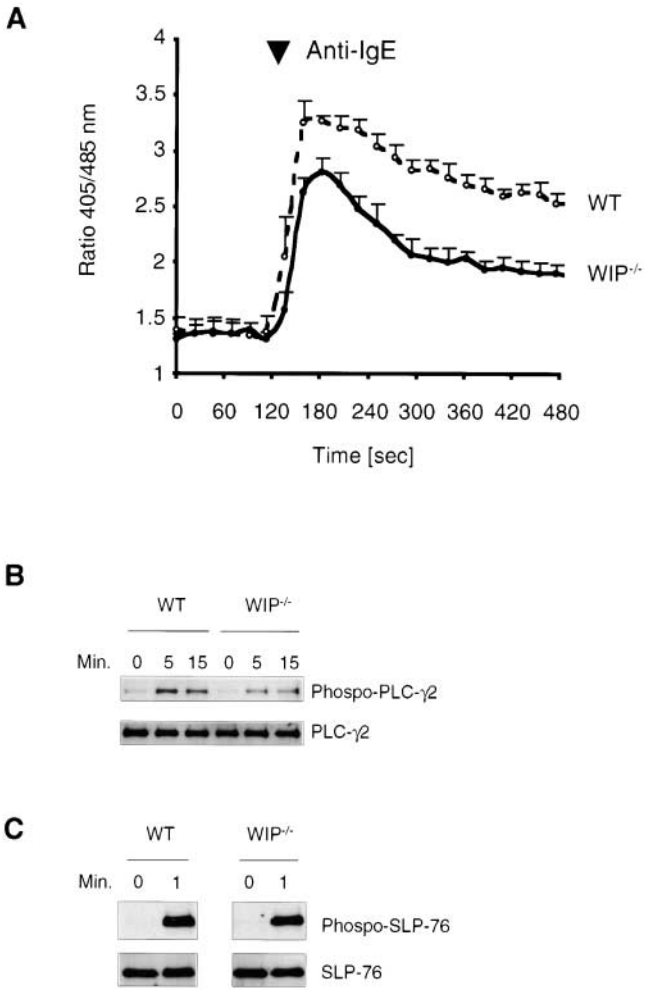

Figure 4. Calcium mobilization and tyrosine phosphorylation of PLC-γ2 in response to FcεRI ligation. (A) Change of fluorescence of the calcium-sensitive dye indo 1-AM was monitored for the indicated time. IgE-sensitized cells were stimulated with F(ab′)$_2$ anti–rat Ig at the indicated time points. Values were plotted as ratio of fluorescence at 405 and 485 nm. (B) Tyrosine phosphorylation of PLC-γ2 in WIP$^{-/-}$ BMMCs. IgE-sensitized BMMCs were activated by FcεRI cross-linking with F(ab′)$_2$ anti–rat Ig for the indicated time at 37°C. Cell lysates were immunoprecipitated with anti–PLC-γ2. PLC-γ2 tyrosine phosphorylation was analyzed by immunoblotting with antiphosphotyrosine antibody. The membrane was reprobed with anti–PLC-γ2 to control for loading. (C) Tyrosine phosphorylation of SLP-76. Cells were stimulated as for PLC-γ2 tyrosine phosphorylation and cell lysates were immunoprecipitated with anti–SLP-76 antibody. The membrane was reprobed with anti–SLP-76 to control for loading.

MAP Kinase Activation in Response to FcεRI Ligation. FcεRI cross-linking induces phosphorylation and activation of the MAP kinases Erk, JNK, and p38 in mast cells (15, 36). The phosphorylation status of the MAP kinases Erk, JNK, and p38 in WIP$^{-/-}$ BMMCs after FcεRI cross-linking was examined by Western blotting with antibodies that recognize selectively these kinases in their phosphorylated state. Phosphorylation of Erk and p38 was minimally affected in WIP$^{-/-}$ mast cells compared with WT controls (Fig. 5, A and B). In contrast, FcεRI-mediated phosphorylation of JNK, both p54 and p46 forms, was reduced and less sustained in WIP$^{-/-}$ mast cells (Fig. 5 C).

Published February 2, 2004

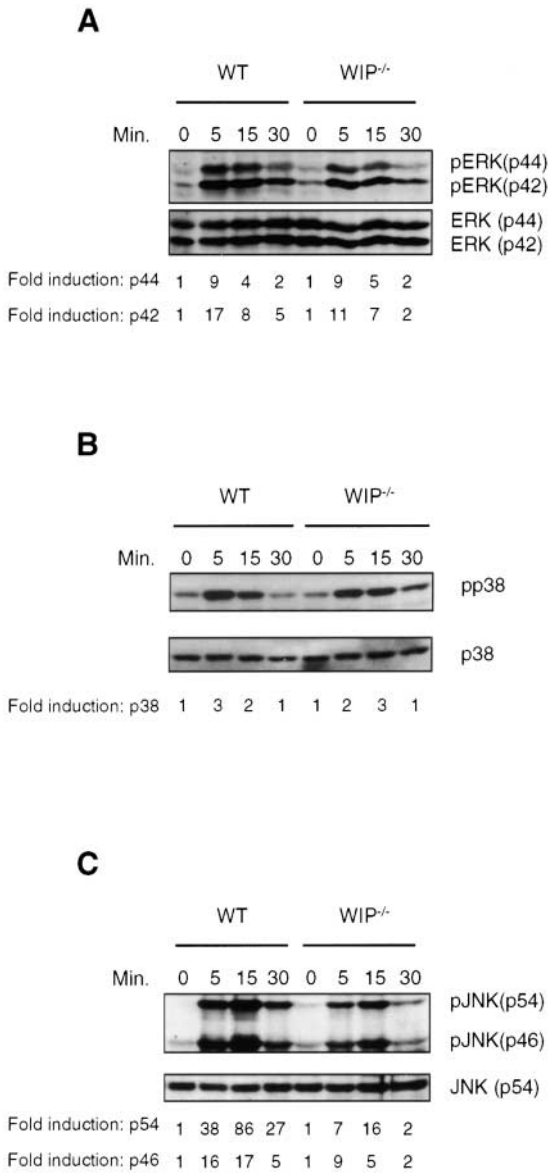

Figure 5. Activation of MAP kinases in response to FcεRI ligation. BMMCs were stimulated for the indicated times and lysed in SDS-PAGE sample buffer. Aliquots of the lysates were analyzed in parallel for phosphorylation of ERK1/2 (A), p38 (B), and SAPK/JNK (C) by Western blotting with the corresponding phospho-specific antibodies. Membranes were reprobed with kinase-specific antibodies to control for loading. Representative blots of three experiments are shown. Mean fold induction ($n = 3$) normalized to signal for loading was determined by densitometry.

WIP Associates with Syk after FcεRI Ligation and Stabilizes Syk Protein. Syk plays a critical role in transmitting signals from FcεRI. The multiple defects in FcεRI signaling in WIP$^{-/-}$ BMMCs prompted us to examine whether WIP is linked to Syk. Phosphorylated Syk is known to associate with the SH2 and SH3 domains containing adaptor protein CrkL via phosphotyrosine–SH2 domain interactions (37). We have recently shown that CrkL directly binds to WIP and that the Syk homologue ZAP-70 associates with WIP after TCR ligation, suggesting that CrkL bridges phosphorylated ZAP-70 to WIP (37). Therefore, we examined whether Syk and WIP associate after FcεRI ligation. WIP immunoprecipitates from lysates of BMMCs from WT mice were probed for Syk before and after FcεRI ligation. There was no detectable Syk in WIP immunoprecipitates from unstimulated cells. FcεRI ligation resulted in the association of Syk with WIP (Fig. 6 A). These results suggest that WIP and Syk are recruited to the same complex in activated BMMCs.

Next, we examined tyrosine phosphorylation of Syk in WIP$^{-/-}$ BMMCs. Initial probing of BMMCs lysates for Syk revealed a severe reduction in Syk protein levels in WIP$^{-/-}$ BMMCs (Fig. 6 B). This decrease was specific to Syk because the levels of actin (Fig. 6 B), PLC-γ2, and SLP-76 (Fig. 4, B and C) were unaffected. FcεRI ligation in WIP$^{-/-}$ BMMCs resulted in the generation of decreased amounts of phosphorylated Syk compared with WT BMMCs (Fig. 6 C). Densitometry analysis revealed that this decrease was commensurate with the decrease in Syk protein levels as evidenced by comparable ratios of intensities of phospho-Syk to total Syk bands after FcεRI ligation in WIP$^{-/-}$ BMMCs and WT controls. These results suggest that WIP is essential for normal Syk protein expression.

The decrease in Syk protein expression was not due to decreased Syk mRNA expression as Syk mRNA levels were comparable in WIP$^{-/-}$ and WT BMMCs as assessed by Northern blot analysis (Fig. 6 D). Syk is subject to ubiquitination by Cbl and subsequent degradation by the proteasome in B cells and mast cells and is also a substrate for calpain (38–40). We examined the effect of proteasome and calpain inhibitors on Syk levels in WIP$^{-/-}$ BMMCs. Pretreatment of WIP$^{-/-}$ BMMCs for 6 h with the calpain inhibitor calpeptin and with the proteasome inhibitor MG132 resulted in an increase in Syk levels, which averaged 2.5 ± 0.6-fold in three experiments (Fig. 6 E). Neither inhibitor alone had a detectable effect. Pretreatment with calpeptin and MG132 caused no increase (1.1 ± 0.3-fold) in Syk levels in WT BMMCs. Taken together, these results suggest that WIP inhibits the degradation of Syk in mast cells.

Spreading of Mast Cells on IgE-coated Slides. T cells spread and extend protrusions when exposed to anti-TCR/CD3–coated surfaces. This process involves actin cytoskeleton reorganization, which is dependent on WASP and WIP (41, 42). Given the role of WIP in actin cytoskeleton organization, we tested the ability of BMMCs from WT and WIP$^{-/-}$ mice to attach and spread on IgE-coated glass coverslips. WT mast cells did not attach to untreated glass slides (not depicted) but adhered to IgE-coated coverslips. WIP$^{-/-}$ mast cells adhered to IgE-coated coverslips equally as well as WT BMMCs (Fig. 7 A). After attachment, a significant proportion of WT BMMCs spread and extended membrane protrusions (Fig. 7, B and C). Preincubation of WT mast cells with the inhibitor of actin polymerization, cytochalasin D, suppressed their spreading on IgE-coated surfaces (Fig. 7, B and C), suggesting that actin polymerization is critical in this process. WIP$^{-/-}$ BMMCs had reduced ability to spread and form protrusions (Fig. 7 C).

Published February 2, 2004

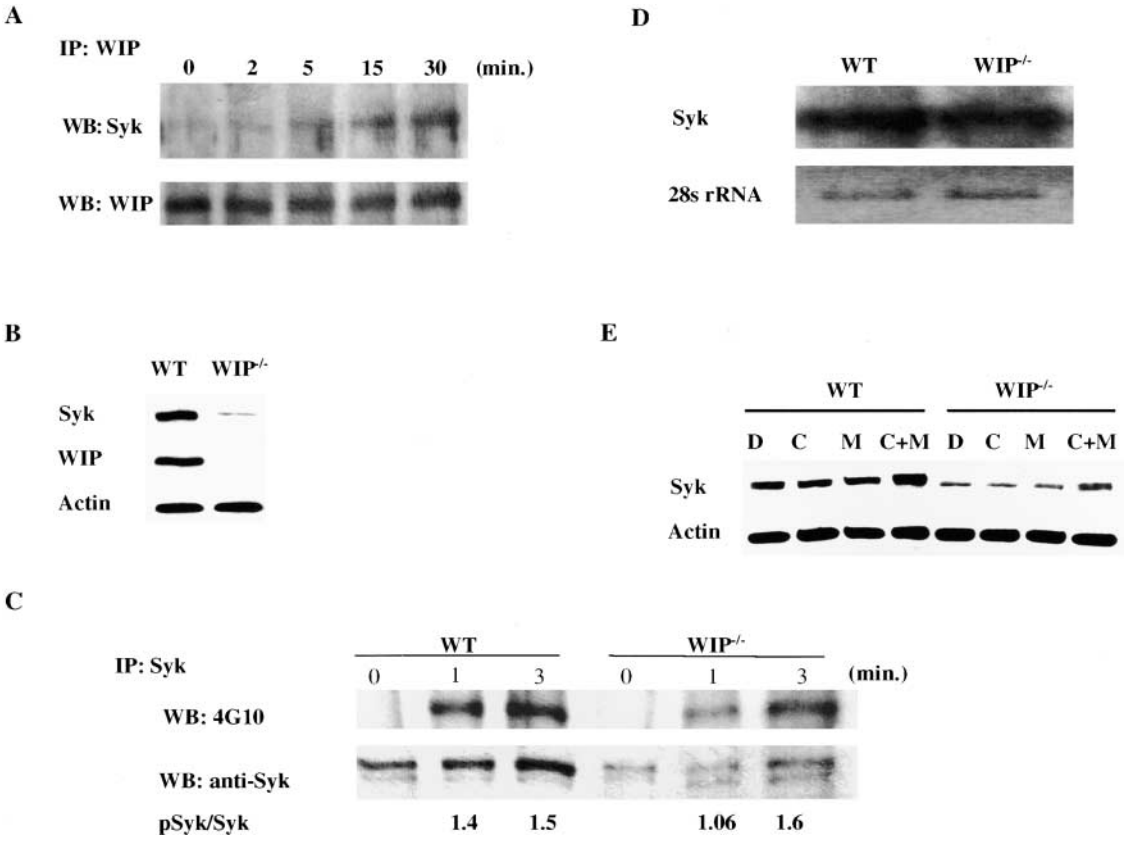

Figure 6. WIP associates with Syk after FcεRI ligation and protects it from degradation. (A) Association of WIP and Syk after FcεRI ligation. WIP immunoprecipitates from WT BMMCs were probed with Syk before and after FcεRI ligation. (B) Syk protein levels in Western blots from lysates of WT and WIP$^{-/-}$ BMMCs. (C) Syk phosphorylation after FcεRI ligation in WT and WIP$^{-/-}$ BMMCs. Syk immunoprecipitates were probed with antiphosphotyrosine mAb 4G10 and with anti-Syk as loading control. Numbers represent densitometric ratio of phopshoSyk to Syk bands. (D) Northern blot analysis of Syk mRNA in WT and WIP$^{-/-}$ BMMCs. 28S RNA is shown as loading control. (E) Effect of pretreatment with calpeptin and MG132 for 6 h on Syk levels in WT and WIP$^{-/-}$ BMMCs.

Electron microscopy revealed that WIP$^{-/-}$ BMMCs that spread on IgE-coated coverslips had no obvious abnormalities in their subcortical actin network (Fig. 7 D). These results suggest that FcεRI-mediated actin polymerization–dependent spreading and protrusion formation is impaired in WIP$^{-/-}$ mast cells.

FcεRI Induction of Changes in F-Actin Content Is Abnormal in WIP$^{-/-}$ BMMCs. FcεRI signaling induces changes in cellular F-actin content in mast cells lines (21, 43). We compared F-actin content in WT and WIP$^{-/-}$ BMMCs after FcεRI ligation. Resting WIP$^{-/-}$ BMMCs had a reduced baseline F-actin content compared with WT BMMCs. The mean reduction of cellular F-actin in WIP$^{-/-}$ BMMCs was 12 ± 2.4% in five experiments ($P < 0.01$). FcεRI ligation in WT BMMCs resulted in an initial decrease in F-actin content, with the maximum decrease being observed after 2 min of stimulation. Subsequently, F-actin content slowly increased but was still lower than baseline 30 min after FcεRI ligation (Fig. 8 A). The rapid decrease of F-actin was found to be dependent on the influx of extracellular calcium as no change of F-actin content was observed in the presence of EGTA and as ionomycin also caused a decrease in F-actin content that was sustained (not depicted). WIP$^{-/-}$ BMMCs exhibited an initial decrease in F-actin that was similar to that observed in WT controls. However, in contrast to what was observed in WT BMMCs, the F-actin content of WIP$^{-/-}$ BMMCs returned almost immediately back to prestimulation level (Fig. 8 A).

To further examine F-actin dynamics, we determined the number of free pointed and barbed ends of F-actin filaments in WT and WIP$^{-/-}$ BMMCs after FcεRI ligation. The number of pointed ends in both types of BMMCs exceeded by 30–40-fold that of barbed ends, suggesting that as expected, the vast majority of barbed ends are capped (Fig. 8 B). FcεRI ligation in WT BMMCs caused rapid generation of both pointed and barbed ends that peaked at 1–2 min, with a progressive decrease in the next 15 min. Unstimulated WIP$^{-/-}$ BMMCs had significantly less pointed ends than WT BMMCs, consistent with their lower baseline content of F-actin. FcεRI ligation in WIP$^{-/-}$ BMMCs caused an increase in the number of pointed ends that was of a similar relative magnitude to that observed in WT BMMCs (Fig. 8 B). This result, together with the comparable decrease in total F-actin content in WIP$^{-/-}$ and WT BMMCs, suggests that actin depolymerization and/or sev-

Published February 2, 2004

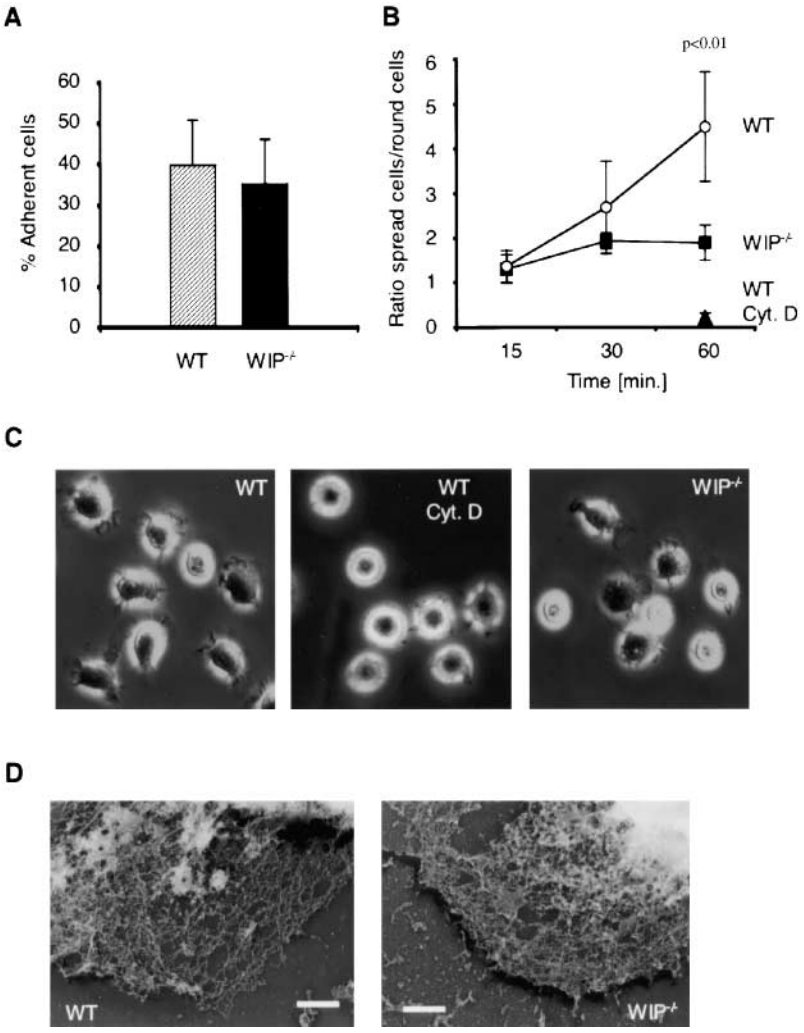

Figure 7. Adhesion and spreading of BMMCs on IgE-coated glass slides. (A) Quantification of BMMCs that adhered to IgE-coated glass coverslips. Cells were incubated for 1 h on IgE-coated glass coverslips. The percentage of adherent cells was then determined by β-hexosaminidase content of attached versus detached cells. (B) Quantification of BMMCs spread on IgE-coated glass coverslips. Cells were fixed at indicated time points and were counted under the microscope (×400) to determine the ratio of round versus spread cells. BMMCs preincubated with cytochalasin D were counted after 1 h of incubation. Results represent ratio of spread/round cells of >500 cells per condition counted from two independent experiments. (C) Representative frames of WT (left), WT treated with cytochalasin D (middle), and WIP$^{-/-}$ (right) BMMCs incubated on IgE-coated glass slides (×400). (D) Cells that adhered to IgE-coated glass coverslips after 1 h of incubation were extracted and cytoskeletons were metal coated. Bars, 1 mm.

ering is not impaired in the absence of WIP. In contrast to WT BMMCs, WIP$^{-/-}$ BMMCs exhibited only a small increase in the number of barbed ends (Fig. 7 B). This result, together with the accelerated return of total F-actin content to normal in WIP$^{-/-}$ BMMCs, suggests that generation and/or elongation and capping of actin filaments proceeds more efficiently in the absence of WIP.

FcεRI Induction of Cell Shape Changes Is Dysregulated in WIP$^{-/-}$ BMMCs. FcεRI signaling evokes changes in cell shape in mast cells (43, 44). Mast cells in the tissue are in contact with proteins of the extracellular matrix. In an attempt to simulate this environment we developed an assay where we allowed the cells to spread on fibronectin-coated glass coverslips and monitored the cell shape dynamics after FcεRI stimulation with video microscopy. BMMCs preincubated with IgE were allowed to spread at 37°C on fibronectin-coated glass coverslips and after an initial observation time of 1 min, the cross-linking antibody was added and cells were monitored for 12 min thereafter (Fig. 8 C). As shown in Fig. 8 C at time 0, both cell types spread and extended membrane protrusions on the fibronectin-coated surface. 2 min after FcεRI cross-linking, both WT and WIP$^{-/-}$ cells had retracted their membrane protrusions and rounded up. This retractile phase lasted 8 min in WT BMMCs, after which the cells started to resume their original spread shape and to extend membrane protrusions. In contrast, the retractile phase was very transient in WIP$^{-/-}$ BMMCs, lasting only ~2 min. These results suggest that WIP regulates the kinetics of recovery of cell shape after the retraction induced by FcεRI ligation.

Discussion

Here we report that mast cells that lack WIP are impaired in their response to FcεRI ligation and provide evidence that WIP controls Syk levels and FcεRI signaling in mast cells and regulates actin cytoskeleton rearrangement triggered by FcεRI ligation.

WIP is not essential for mast cell growth and differentiation in vivo and in vitro as equal numbers of tissue mast cells were detected in ears of WIP$^{-/-}$ mice and the differentiation and development of BMMCs of WIP$^{-/-}$ mice in vitro were normal. Mast cell development is mainly driven by IL-3 (23) and other cytokines such as stem cell factor

Published February 2, 2004

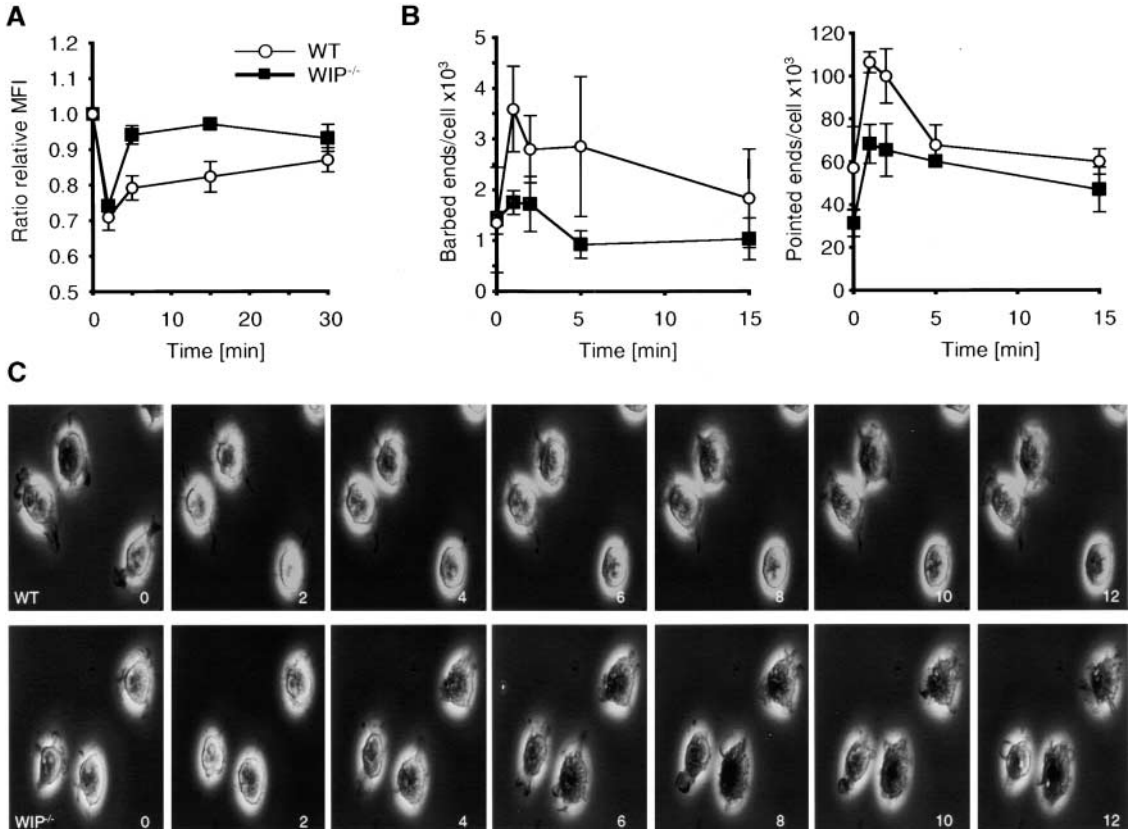

Figure 8. Determination of cellular F-actin and time lapse video microscopy of BMMCs activated by FcεRI ligation. (A) IgE-sensitized BMMCs were stimulated by cross-linking of FcεRI for the indicated time. Cells were then fixed, permeabilized, stained with phalloidin-TRITC, and analyzed by FACS®. Results represent mean ± SD of three experiments. (B) Barbed and pointed end counts of activated BMMCs determined by pyrene-labeled actin assembly assay. (C) IgE-sensitized BMMCs were allowed to attach to fibronectin-coated glass coverslips for 20 min at 37°C. Cells were then videotaped for 15 min and FcεRI cross-linking was induced after 1 min (frame 0). The indicated time frames were processed using NIH Image software. ×400.

(45), but is thought not to be dependent on signals from FcεRI as it proceeds normally in FcεRIα$^{-/-}$ mice (31).

WIP-deficient mice were resistant to IgE-mediated systemic histamine release, an event which has been shown to be dependent both on mast cells and FcεRI signaling (28–31). Because the plasma histamine levels in these mice after intravenous antigen challenge remained low as compared with WT controls, we conclude that WIP is a critical component of the FcεRI signaling pathway.

BMMCs isolated from WIP-deficient mice released significantly less β-hexosaminidase and produced lower amounts of IL-6 after FcεRI ligation than BMMCs derived from WT littermates. Considered, respectively, as early and late events triggered by ligation of the FcεRI, degranulation and IL-6 production both depend on increased and sustained intracellular calcium levels. Upon FcεRI cross-linking, intracellular calcium levels were lower and less sustained in WIP$^{-/-}$ BMMCs as compared with WT cells. The rise of intracellular calcium concentration is dependent on the activation of PLC-γ. In accordance, PLC-γ2 tyrosine phosphorylation was reduced in WIP$^{-/-}$ cells.

Propagation of the FcεRI signal is dependent on Syk. WIP was found to associate with Syk after FcεRI ligation. This is consistent with our previous finding that WIP associates with ZAP-70 after TCR ligation (24). It is likely that the association of WIP with Syk is mediated by the adaptor protein CrkL. CrkL directly and constitutively binds to WIP via SH3 domain–proline-rich region interactions and is recruited to phosphorylated Syk via SH2 domain–phosphotyrosine interactions (24, 37). This may result in the formation of an Syk–CrkL–WIP complex after FcεRI ligation. Our data strongly suggests that WIP inhibits the degradation of Syk. Syk protein levels, but not Syk mRNA levels, were selectively diminished in WIP$^{-/-}$ BMMCs. Diminished Syk levels and the subsequent decrease in phospho-Syk levels after FcεRI ligation in WIP$^{-/-}$ BMMCs probably contributes to impaired FcεRI signaling in these cells. The observation that phosphorylation of PLC-γ2, but not of SLP-76, was diminished in WIP$^{-/-}$ BMMCs suggests that tyrosine kinases other than Syk may participate in SLP-76 phosphorylation after FcεRI ligation.

After FcεRI ligation, Cbl is recruited to Syk and phosphorylated. This causes it to ubiquinate Syk, targeting it for degradation by the proteasome (38, 40). Phosphorylated Cbl can recruit CrkL via interaction with its SH2 domain (46, 47). This may result in the formation of an Syk–Cbl–CrkL–WIP complex. Furthermore, Syk is a target for degradation by calpain (48). This may occur in lipid rafts

Published February 2, 2004

where activated Syk is recruited and where calpain is present constitutively (not depicted). The diminished level of Syk in WIP-deficient mast cells and its partial rescue by calpain and proteasome inhibitors suggest that WIP may interfere with Cbl ubiquitination of Syk and with its degradation by calpain. The requirement for both calpain and proteasome inhibitors for this rescue suggests that calpain and the ubiquitin/proteasome pathway synergize in degrading Syk in $WIP^{-/-}$ mast cells.

IL-6 production after FcεRI cross-linking has been shown to be strongly linked to JNK activation in mast cells (49, 50). The impaired capacity of $WIP^{-/-}$ to produce IL-6 in response to FcεRI ligation was paralleled by reduced phosphorylation of JNK kinase observed in these cells. WIP could potentially modulate JNK activation via its effect on actin polymerization, as JNK has been shown to be regulated by the actin cytoskeleton (51). Alternatively, WIP, through its interaction with WASP, might induce transcriptional activation independent of actin polymerization as it has been proposed in T cells (12).

WIP-deficient BMMCs adhered to IgE-coated coverslips and undergo similar morphological changes as WT cells, although the number of cells that spread after 1 h of incubation was significantly decreased. IgE-induced spreading was dependent on actin polymerization as it was inhibited by cytochalasin D. Electron microscopy revealed that $WIP^{-/-}$ cells that spread had the same pattern of cortical actin network as WT cells, indicating that actin polymerization involved in the formation of motile protrusions in mast cells is unaffected by lack of $WIP^{-/-}$. This finding was surprising because T and B cells from WIP-deficient mice display abnormal cortical actin networks when they are incubated on anti-TCR– or anti–B cell receptor–coated coverslips (13). These results suggest that actin polymerization is differently regulated in mast cells after FcεRI ligation compared with TCR engagement in T cells and surface IgM cross-linking in B cells. TCR and B cell receptor ligation triggers actin polymerization in T and B cells reflected by an increase of F-actin content (52). In contrast, F-actin content rapidly decreased in mast cells after FcεRI ligation. This initial decrease in F-actin content was followed by a subsequent gradual increase of F-actin to almost prestimulation levels. Using time lapse video microscopy, we were able to follow the morphological changes triggered by FcεRI ligation in BMMCs that were allowed to spread on fibronectin-coated glass coverslips. Upon stimulation, these changes consisted of an initial rounding of the cells followed by a slow resumption of the spread state in WT BMMCs. The kinetics of these changes paralleled those observed in the F-actin content, suggesting that BMMCs rapidly depolymerize F-actin after FcεRI ligation followed by a phase of actin polymerization. Furthermore, these results are in accordance with the findings that the increase in the number of pointed ends after FcεRI ligation were comparable in $WIP^{-/-}$ and WT BMMCs, suggesting that actin depolymerization and/or severing is not impaired in the absence of WIP. Experiments with permeabilized mast cells have suggested that in the early phase of the degranulation process actin is depolymerized or severed (53–55). Furthermore, mast cell degranulation is enhanced in the presence of cytochalasin D and latrunculin, inhibitors that disrupt actin microfilaments without causing degranulation per se (21, 22). The disassembly of cortical actin has been shown to be dependent on calcium and involved the actin filament severing and capping protein gelsolin and Rho GTPases (53–56). The small Rho family GTPases Rac and Cdc42 have been shown to regulate mast cell function. GTP-Cdc42 binds to WASP and activates its ability to interact with the Arp2/3 complex and to induce actin polymerization (57–59). WIP retards N-WASP/Cdc42–activated actin polymerization (60). Furthermore, we have recently shown that TCR ligation results in protein kinase C θ–mediated phosphorylation of WIP and its subsequent dissociation from WASP might be required for F-actin accumulation in T cells (24). This dissociation releases WASP from the inhibitory effect of WIP, allowing it to get activated by Cdc42. Thus, in the absence of WIP, WASP-mediated actin polymerization might progress more rapidly. This regulatory role for WIP may explain our results that WIP-deficient BMMCs increase their F-actin content more rapidly after FcεRI ligation and remain in the retracted state for a shorter time than WT BMMCs. Alternatively, WIP may regulate actin polymerization directly. The observation that $WIP^{-/-}$ BMMCs exhibited only a small increase in the number of barbed ends after FcεRI ligation suggests that barbed ends are more efficiently capped and/or that filaments are more efficiently elongated in the absence of WIP. This would then result in accelerated return of total F-actin content to normal.

In summary, our findings suggest that WIP regulates IgE-dependent mast cell activation by regulating Syk levels, FcεRI signaling, and actin cytoskeletal reorganization, and may represent potential therapeutic targets in allergic diseases.

We thank D. Laouini for assistance in growing mast cells and in the in vivo histamine release experiment and N. Ramesh and H. Oettgen for critical evaluation of the manuscript.

This work is supported by U.S. Public Health Service grant AI-35714, by research grants from the Hood Foundation and the Baxter, Aventis, and Gentiva Corporations, a Swiss National Science Foundation research fellowship, and an American Academy of Allergy Asthma and Immunology Zeneca Research Award (to A. Kettner).

Submitted: 22 April 2003
Accepted: 5 December 2003

References

1. Derry, J.M.J., H.D. Ochs, and U. Francke. 1994. Isolation of a novel gene mutated in Wiskott-Aldrich syndrome. *Cell.* 78: 635–644.
2. Kenney, D., L. Cairns, E. Remold-O'Donnell, J. Peterson, F.S. Rosen, and R. Parkman. 1986. Morphological abnormalities in the lymphocytes of patients with the Wiskott-Aldrich syndrome. *Blood.* 68:1329–1332.
3. Binks, M., G.E. Jones, P.M. Brickell, C. Kinnon, D.R. Katz, and A.J. Thrasher. 1998. Intrinsic dendritic cell abnormalities in Wiskott-Aldrich syndrome. *Eur. J. Immunol.* 28:3259–

3267.
4. Gallego, M.D., M. Santamaria, J. Pena, and I.J. Molina. 1997. Defective actin reorganization and polymerization of Wiskott-Aldrich T cells in response to CD3-mediated stimulation. *Blood.* 90:3089–3097.
5. Molina, I.J., J. Sancho, C. Terhorst, F.S. Rosen, and E. Remold-O'Donnell. 1993. T cells of patients with the Wiskott-Aldrich syndrome have a restricted defect in proliferative responses. *J. Immunol.* 151:4383–4390.
6. Zicha, D., W.E. Allen, P.M. Brickell, C. Kinnon, G.A. Dunn, G.E. Jones, and A.J. Thrasher. 1998. Chemotaxis of macrophages is abolished in the Wiskott-Aldrich syndrome. *Br. J. Haematol.* 101:659–665.
7. Snapper, S.B., F.S. Rosen, E. Mizoguchi, P. Cohen, W. Khan, C.H. Liu, T.L. Hagemann, S.P. Kwan, R. Ferrini, L. Davidson, et al. 1998. Wiskott-Aldrich syndrome protein-deficient mice reveal a role for WASP in T but not B cell activation. *Immunity.* 9:81–91.
8. Zhang, J., A. Shehabeldin, L.A. da Cruz, J. Butler, A.K. Somani, M. McGavin, I. Kozieradzki, A.O. dos Santos, A. Nagy, S. Grinstein, et al. 1999. Antigen receptor–induced activation and cytoskeletal rearrangement are impaired in Wiskott-Aldrich syndrome protein–deficient lymphocytes. *J. Exp. Med.* 190:1329–1342.
9. Ramesh, N., I.M. Anton, J.H. Hartwig, and R.S. Geha. 1997. WIP, a protein associated with the Wiskott-Aldrich syndrome protein, induces actin polymerization and redistribution in lymphoid cells. *Proc. Natl. Acad. Sci. USA.* 94: 14671–14676.
10. Schwarz, K., S. Nonoyama, M. Peitsch, G. de Saint Basile, T. Espanol, A. Fasth, A. Fischer, K. Freitag, W. Friedrich, S. Fugmann, et al. 1996. WASPbase: a database of WAS- and XLT-causing mutations. *Immunol. Today.* 17:496–502.
11. Stewart, D.M., L. Tian, and D.L. Nelson. 1999. Mutations that cause the Wiskott-Aldrich syndrome impair the interaction of Wiskott-Aldrich syndrome protein (WASP) with WASP interacting protein. *J. Immunol.* 162:5019–5024.
12. Savoy, D.N., D.D. Billadeau, and P.J. Leibson. 2000. WIP, a binding partner for Wiskott-Aldrich syndrome protein, cooperates with Vav in the regulation of T cell activation. *J. Immunol.* 164:2866–2870.
13. Anton, I.M., M.A. de la Fuente, T.N. Sims, S. Freeman, N. Ramesh, J.H. Hartwig, M.L. Dustin, and R.S. Geha. 2002. WIP deficiency reveals a differential role for WIP and the actin cytoskeleton in T and B cell activation. *Immunity.* 16:193–204.
14. Blank, U., C. Ra, L. Miller, K. White, H. Metzger, and J.-P. Kinet. 1989. Complete structure and expression in transfected cells of high affinity IgE receptor. *Nature.* 337:187–189.
15. Kinet, J.P., M.H. Jouvin, R. Paolini, R. Numerof, and A. Scharenberg. 1996. IgE receptor (Fc epsilon RI) and signal transduction. *Eur. Respir. J. Suppl.* 22:116s–118s.
16. Hendricks-Taylor, L.R., D.G. Motto, J. Zhang, R.P. Siraganian, and G.A. Koretzky. 1997. SLP-76 is a substrate of the high affinity IgE receptor-stimulated protein tyrosine kinases in rat basophilic leukemia cells. *J. Biol. Chem.* 272:1363–1367.
17. Costello, P.S., M. Turner, A.E. Walters, C.N. Cunningham, P.H. Bauer, J. Downward, and V.L. Tybulewicz. 1996. Critical role for the tyrosine kinase Syk in signalling through the high affinity IgE receptor of mast cells. *Oncogene.* 13:2595–2605.
18. Margolis, B., P. Hu, S. Katzav, W. Li, J.M. Oliver, A. Ullrich, A. Weiss, and J. Schlessinger. 1992. Tyrosine phosphorylation of vav proto-oncogene product containing SH2 domain and transcription factor motifs. *Nature.* 356:71–74.
19. Apgar, J.R. 1990. Antigen-induced cross-linking of the IgE receptor leads to an association with the detergent-insoluble membrane skeleton of rat basophilic leukemia (RBL-2H3) cells. *J. Immunol.* 145:3814–3822.
20. Apgar, J.R. 1995. Activation of protein kinase C in rat basophilic leukemia cells stimulates increased production of phosphatidylinositol 4-phosphate and phosphatidylinositol 4,5-bisphosphate: correlation with actin polymerization. *Mol. Biol. Cell.* 6:97–108.
21. Frigeri, L., and J.R. Apgar. 1999. The role of actin microfilaments in the down-regulation of the degranulation response in RBL-2H3 mast cells. *J. Immunol.* 162:2243–2250.
22. Holowka, D., E.D. Sheets, and B. Baird. 2000. Interactions between Fc(epsilon)RI and lipid raft components are regulated by the actin cytoskeleton. *J. Cell Sci.* 113:1009–1019.
23. Razin, E., J.N. Ihle, D. Seldin, J.M. Mencia-Huerta, H.R. Katz, P.A. LeBlanc, A. Hein, J.P. Caulfield, K.F. Austen, and R.L. Stevens. 1984. Interleukin 3: a differentiation and growth factor for the mouse mast cell that contains chondroitin sulfate E proteoglycan. *J. Immunol.* 132:1479–1486.
24. Sasahara, Y., R. Rachid, M.J. Byrne, M.A. de la Fuente, R.T. Abraham, N. Ramesh, and R.S. Geha. 2002. Mechanism of recruitment of WASP to the immunological synapse and of its activation following TCR ligation. *Mol. Cell.* 10: 1269–1281.
25. Kumar, L., V. Pivniouk, and R.S. Geha. 2002. Role of SLP-76 domains in T cell development and function. *Proc. Natl. Acad. Sci. USA.* 99:884–889.
26. Hartwig, J.H., and M. DeSisto. 1991. The cytoskeleton of the resting human blood platelet: structure of the membrane skeleton and its attachment to actin filaments. *J. Cell Biol.* 112:407–425.
27. Hartwig, J.H. 1992. Mechanisms of actin rearrangements mediating platelet activation. *J. Cell Biol.* 118:1421–1442.
28. Takeishi, T., T.R. Martin, I.M. Katona, F.D. Finkelman, and S.J. Galli. 1991. Differences in the expression of the cardiopulmonary alterations associated with anti-immunoglobulin E-induced or active anaphylaxis in mast cell-deficient and normal mice. Mast cells are not required for the cardiopulmonary changes associated with certain fatal anaphylactic responses. *J. Clin. Invest.* 88:598–608.
29. Martin, T.R., A. Ando, T. Takeishi, I.M. Katona, J.M. Drazen, and S.J. Galli. 1993. Mast cells contribute to the changes in heart rate, but not hypotension or death, associated with active anaphylaxis in mice. *J. Immunol.* 151:367–376.
30. Ando, A., T.R. Martin, and S.J. Galli. 1993. Effects of chronic treatment with the c-kit ligand, stem cell factor, on immunoglobulin E-dependent anaphylaxis in mice. Genetically mast cell-deficient Sl/Sld mice acquire anaphylactic responsiveness, but the congenic normal mice do not exhibit augmented responses. *J. Clin. Invest.* 92:1639–1649.
31. Dombrowicz, D., V. Flamand, K.K. Brigman, B.H. Koller, and J.-P. Kinet. 1993. Abolition of anaphylaxis by targeted disruption of the high affinity immunoglobulin E receptor alpha chain gene. *Cell.* 75:969–976.
32. Oettgen, H.C., T.R. Martin, A. Wynshaw-Boris, C. Deng, J.M. Drazen, and P. Leder. 1994. Active anaphylaxis in IgE-deficient mice. *Nature.* 370:367–370.
33. Park, D.J., H.K. Min, and S.G. Rhee. 1991. IgE-induced ty-

rosine phosphorylation of phospholipase C-gamma 1 in rat basophilic leukemia cells. *J. Biol. Chem.* 266:24237–24240.
34. Zhang, J., E.H. Berenstein, R.L. Evans, and R.P. Siraganian. 1996. Transfection of Syk protein tyrosine kinase reconstitutes high affinity IgE receptor–mediated degranulation in a Syk-negative variant of rat basophilic leukemia RBL-2H3 cells. *J. Exp. Med.* 184:71–79.
35. Wen, R., S.T. Jou, Y. Chen, A. Hoffmeyer, and D. Wang. 2002. Phospholipase C gamma 2 is essential for specific functions of Fc epsilon R and Fc gamma R. *J. Immunol.* 169: 6743–6752.
36. Hirasawa, N., F. Santini, and M.A. Beaven. 1995. Activation of the mitogen-activated protein kinase/cytosolic phospholipase A2 pathway in a rat mast cell line. Indications of different pathways for release of arachidonic acid and secretory granules. *J. Immunol.* 154:5391–5402.
37. Oda, A., H.D. Ochs, L.A. Lasky, S. Spencer, K. Ozaki, M. Fujihara, M. Handa, K. Ikebuchi, and H. Ikeda. 2001. CrkL is an adapter for Wiskott-Aldrich syndrome protein and Syk. *Blood.* 97:2633–2639.
38. Paolini, R., R. Molfetta, L.O. Beitz, J. Zhang, A.M. Scharenberg, M. Piccoli, L. Frati, R. Siraganian, and A. Santoni. 2002. Activation of Syk tyrosine kinase is required for c-Cbl-mediated ubiquitination of Fcepsilon RI and Syk in RBL cells. *J. Biol. Chem.* 277:36940–36947.
39. Rao, N., A.K. Ghosh, S. Ota, P. Zhou, A.L. Reddi, K. Hakezi, B.K. Druker, J. Wu, and H. Band. 2001. The nonreceptor tyrosine kinase Syk is a target of Cbl-mediated ubiquitylation upon B-cell receptor stimulation. *EMBO J.* 20: 7085–7095.
40. Youssef, L.A., B.S. Wilson, and J.M. Oliver. 2002. Proteasome-dependent regulation of Syk tyrosine kinase levels in human basophils. *J. Allergy Clin. Immunol.* 110:366–373.
41. Parsey, M.V., and G.K. Lewis. 1993. Actin polymerization and pseudopod reorganization accompany anti-CD3-induced growth arrest in Jurkat cells. *J. Immunol.* 151:1881–1893.
42. Bunnell, S.C., V. Kapoor, R.P. Trible, W. Zhang, and L.E. Samelson. 2001. Dynamic actin polymerization drives T cell receptor-induced spreading a role for the signal transduction adaptor LAT. *Immunity.* 14:315–329.
43. Pfeiffer, J.R., J.C. Seagrave, B.H. Davis, G.G. Deanin, and J.M. Oliver. 1985. Membrane and cytoskeletal changes associated with IgE-mediated serotonin release from rat basophilic leukemia cells. *J. Cell Biol.* 101:2145–2155.
44. Dvorak, A.M., E.S. Schulman, S.P. Peters, D.W. MacGlashan, Jr., H.H. Newball, R.P. Schleimer, and L.M. Lichtenstein. 1985. Immunoglobulin E-mediated degranulation of isolated human lung mast cells. *Lab. Invest.* 53:45–56.
45. Tsai, M., L.S. Shih, G.F. Newlands, T. Takeishi, K.E. Langley, K.M. Zsebo, H.R. Miller, E.N. Geissler, and S.J. Galli. 1991. The rat c-kit ligand, stem cell factor, induces the development of connective tissue-type and mucosal mast cells in vivo. Analysis by anatomical distribution, histochemistry, and protease phenotype. *J. Exp. Med.* 174:125–131.
46. Reedquist, K.A., T. Fukazawa, G. Panchamoorthy, W.Y. Langdon, S.E. Shoelson, B.J. Druker, and H. Band. 1996. Stimulation through the T cell receptor induces Cbl association with Crk proteins and the guanine nucleotide exchange protein C3G. *J. Biol. Chem.* 271:8435–8442.
47. Bhat, A., K. Kolibaba, T. Oda, S. Ohno-Jones, C. Heaney, and B.J. Druker. 1997. Interactions of CBL with BCR-ABL and CRKL in BCR-ABL-transformed myeloid cells. *J. Biol. Chem.* 272:16170–16175.
48. Baldock, D., B. Graham, M. Akhlaq, P. Graff, C.E. Jones, and K. Menear. 2000. Purification and characterization of human Syk produced using a baculovirus expression system. *Protein Expr. Purif.* 18:86–94.
49. Arudchandran, R., M.J. Brown, M.J. Peirce, J.S. Song, J. Zhang, R.P. Siraganian, U. Blank, and J. Rivera. 2000. The Src homology 2 domain of Vav is required for its compartmentation to the plasma membrane and activation of c-Jun NH_2-terminal kinase 1. *J. Exp. Med.* 191:47–60.
50. Song, J.S., H. Haleem-Smith, R. Arudchandran, J. Gomez, P.M. Scott, J.F. Mill, T.H. Tan, and J. Rivera. 1999. Tyrosine phosphorylation of Vav stimulates IL-6 production in mast cells by a Rac/c-Jun N-terminal kinase-dependent pathway. *J. Immunol.* 163:802–810.
51. Oren, A., A. Herschkovitz, I. Ben-Dror, V. Holdengreber, Y. Ben-Shaul, R. Seger, and L. Vardimon. 1999. The cytoskeletal network controls c-Jun expression and glucocorticoid receptor transcriptional activity in an antagonistic and cell-type-specific manner. *Mol. Cell. Biol.* 19:1742–1750.
52. Phatak, P.D., and C.H. Packman. 1994. Engagement of the T-cell antigen receptor by anti-CD3 monoclonal antibody causes a rapid increase in lymphocyte F-actin. *J. Cell. Physiol.* 159:365–370.
53. Sullivan, R., M. Burnham, K. Torok, and A. Koffer. 2000. Calmodulin regulates the disassembly of cortical F-actin in mast cells but is not required for secretion. *Cell Calcium.* 28: 33–46.
54. Borovikov, Y.S., J.C. Norman, L.S. Price, A. Weeds, and A. Koffer. 1995. Secretion from permeabilised mast cells is enhanced by addition of gelsolin: contrasting effects of endogenous gelsolin. *J. Cell Sci.* 108:657–666.
55. Norman, J.C., L.S. Price, A.J. Ridley, A. Hall, and A. Koffer. 1994. Actin filament organization in activated mast cells is regulated by heterotrimeric and small GTP-binding proteins. *J. Cell Biol.* 126:1005–1015.
56. Price, L.S., J.C. Norman, A.J. Ridley, and A. Koffer. 1995. The small GTPases Rac and Rho as regulators of secretion in mast cells. *Curr. Biol.* 5:68–73.
57. Kim, A.S., L.T. Kakalis, N. Abdul-Manan, G.A. Liu, and M.K. Rosen. 2000. Autoinhibition and activation mechanisms of the Wiskott-Aldrich syndrome protein. *Nat. Cell Biol.* 404:151–158.
58. Miki, H., T. Sasaki, Y. Takai, and T. Takenawa. 1998. Induction of filopodium formation by a WASP-related actin-depolymerizing protein N-WASP. *Nature.* 391:93–96.
59. Rohatgi, R., L. Ma, H. Miki, M. Lopez, T. Kirchhausen, T. Takenawa, and M.W. Kirschner. 1999. The interaction between N-WASP and the Arp2/3 complex links Cdc42-dependent signals to actin assembly. *Cell.* 97:221–231.
60. Martinez-Quiles, N., R. Rohatgi, I.M. Anton, M. Medina, S.P. Saville, H. Miki, H. Yamaguchi, T. Takenawa, J.H. Hartwig, R.S. Geha, et al. 2001. WIP regulates N-WASP-mediated actin polymerization and filopodium formation. *Nat. Cell Biol.* 3:484–491.